

# Continuum theory of swelling material surfaces with applications to thermo-responsive gel membranes and surface mass transport

Alessandro Lucantonio<sup>a</sup>, Luciano Teresi<sup>b</sup>, Antonio DeSimone<sup>a,\*</sup>

<sup>a</sup>*SISSA - International School for Advanced Studies, via Bonomea 265, 34136 Trieste - Italy*

<sup>b</sup>*LaMS - Modelling and Simulation Lab, Università Roma Tre, via della Vasca Navale 84, 00146 Roma - Italy*

---

## Abstract

Soft membranes are commonly employed in shape-morphing applications, where the material is programmed to achieve a target shape upon activation by an external trigger, and as coating layers that alter the surface properties of bulk materials, such as the properties of spreading and absorption of liquids. In particular, polymer gel membranes experience swelling or shrinking when their solvent content change and the non-homogeneous swelling field may be exploited to control their shape. Here, we develop a theory of swelling material surfaces to model polymer gel membranes and demonstrate its features by studying numerically applications in the contexts of biomedicine, micro-motility, and coating technology. We also specialize the theory to thermo-responsive gels, which are made of polymers that change their affinity with a solvent when temperature varies.

**Keywords:** material surface, polymer gel, membrane, swelling, drug delivery, micro-motility, spreading

---

## 1. Introduction

Among soft active materials, *i.e.* materials that respond with a mechanical deformation to a non-mechanical stimulus (electrical field, exposure to a solvent, pH change, temperature field), polymer gels play a major role in the current research on novel micro- and nano-devices. The mechanical characteristics of these materials closely resemble those of biological tissues and thus make them candidates for biomedical applications and for bio-inspired devices (Ottenbrite et al., 2010).

In many applications, gels are employed in the form of membranes (Stuart et al., 2010; Ionov, 2011); in particular, in self-shaping materials, these membranes can undergo prescribed three-dimensional shape transformations, by exploiting suitable spatial modulations of the local degree of swelling. The non-uniform swelling field may be obtained through a non-homogeneous in-plane (Klein et al., 2007; Kim et al., 2012; Wu et al., 2013) or through-the-thickness (Hu et al., 1998; Sawa et al., 2010; Lucantonio et al., 2014a) distribution of the cross-linking density or by a localized exposure of the swelling structure to the solvent (Holmes et al., 2011; Lucantonio and Nardinocchi, 2012; Pandey and Holmes, 2013). Alternatively, the shape of a swelling membrane may be manipulated by harnessing the multiphysics coupling between mechanics and solvent transport, specifically through the combination of solvent stimulation with an applied pre-stretch (Lucantonio et al., 2014b,c). Apart from shape-morphing applications, polymer gels have been

---

\*Corresponding author.

Email address: [desimone@sissa.it](mailto:desimone@sissa.it) (Antonio DeSimone)

most successfully employed as drug delivery systems over the past few decades (Hoare and Kohane, 2008). Among the many designs that have been proposed, in reservoir systems the drug core is confined by a spherical gel membrane, which is occasionally made of a stimuli-responsive material, such as a thermo-responsive gel, in order to achieve a pulsatile drug delivery (Peppas et al., 2000; Kikuchi and Okano, 2002). Moreover, boundary surfaces of homogeneous gels exhibit transport properties that differ from those of the bulk material and affect surface phenomena, such as spreading and absorption of liquids (Starov et al., 2002).

Motivated by these applications in diverse and emerging fields, here we study a polymer gel membrane that undergoes swelling when exposed to a solvent. We model such a membrane as a *swelling material surface*, an extension to swelling materials of the concept of material surface, which dates back to (Gurtin and Murdoch, 1975) and involves, in general, a surface endowed with a physical structure ruled by a set of balance equations (balance of mass, forces, moments, energy, ...). In particular, we model the coupled solvent transport and polymer elasticity and introduce a thickness microstructural variable that accounts for the volume change caused by the absorption of solvent. In (McBride et al., 2011) a nonlinear continuum thermomechanics formulation that accounts for surface structures and includes the effects of diffusion and viscoelasticity was presented, and afterwards numerically implemented (Javili et al., 2014). Other relevant works where the theory of material surfaces has been extended to include surface mass transport are (Ganghoffer and Haussy, 2005; Steinmann et al., 2012). However, the volume change associated to solvent absorption (swelling) has not been considered, and a very limited number of applications has been presented, none concerning soft active materials, in general, or polymer gels, in particular. Here, we focus on coating gel membranes, that is, we model swelling material surfaces that cover the boundary of a body and study several systems with relevant applications in the contexts of biomedicine and micro-motility. The theory is sufficiently general to be applicable to stand-alone soft membranes, even in the absence of swelling.

We adopt a direct approach in the formulation of the governing equations for the surface, instead of deducing them from a three-dimensional theory. Precisely, we prescribe a virtual work functional for the surface and use it as a tool to derive the balance of forces and moments. A deductive approach, instead, is employed for the swelling constraint that relates the solvent volume fraction to the volume change of the membrane and for the derivation of the surface free energy, because both involve the notion of volume change caused by solvent migration, which pertains to a three-dimensional body. We obtain a thermodynamically consistent theory that fits in the theoretical framework for swelling gels set in (Lucantonio et al., 2013).

The paper is organized as follows. In Section 2, we set the notation, the kinematics and recall some tools from differential geometry and tensor calculus on surfaces, following (Gurtin and Murdoch, 1975; Murdoch, 1990). In Section 3, we collect the balance equations that govern the coupled elasticity-solvent migration for a three-dimensional body and for a boundary material surface subject to swelling, together with the kinematic constraints that relate the volume change to the solvent uptake. In Section 4, we deal with thermodynamics issues and specify the representation forms for the free energy of the body and the swelling material surface that are suitable for the study of swelling gels. In Section 5, we present the weak formulation of the governing equations of the model, in order to enable their implementation in a finite element solver. Finally, in Section 6, we discuss applications of the theory to a smart drug delivery system, a temperature-activated gel micro-crawler, and to a coated gel that exhibits a competition between surface spreading and absorption of a liquid.

## 2. Preliminaries: notation and kinematics

We consider as a reference scenario a soft membrane swollen with a liquid solvent that lies on the boundary of a three-dimensional body, also made of a soft, swellable material. Both the membrane and the body undergo swelling or shrinking when their solvent content changes. We model the (three-dimensional) membrane as a material surface with a scalar microstructure that measures the thickness variation. We assume that the material surface  $\mathcal{S} \subseteq \partial\mathcal{B}$  covers part (or all) of the boundary  $\partial\mathcal{B}$  of the body  $\mathcal{B} \subset \mathcal{E}$ , where  $\mathcal{E}$  is the three-dimensional Euclidean space whose translation space is  $\mathcal{V}$ . The elements (material points) of the sets  $\mathcal{B}$  and  $\mathcal{S}$  will be labelled with  $X$ . The manifolds  $\mathcal{B}$  and  $\mathcal{S}$  also identify the reference configurations for the body and the material surface, *i.e.* material points are identified with the places they occupy in the reference configuration.

Upon introducing the time  $t \in \mathcal{I} \subset \mathbb{R}$ , we denote by  $f : \mathcal{B} \times \mathcal{I} \rightarrow \mathcal{E}$  the motion of the body, that is a one-parameter family of (smooth injective) deformation mappings such that  $x = f(X, t) \in \mathcal{E}$ . We assume that the boundary material surface is always bonded to the body, so that the motion of the boundary surface  $f_s$  is given by the restriction  $f|_{\mathcal{S}}$  of the motion  $f$ . The images  $\mathcal{B}_t = f(\mathcal{B}, t)$  and  $\mathcal{S}_t = f(\mathcal{S}, t)$  of  $\mathcal{B}$  and  $\mathcal{S}$  under  $f$  are the current configurations of  $\mathcal{B}$  and  $\mathcal{S}$  at time  $t$ , respectively. A superposed dot denotes differentiation with respect to time, which is regarded as a parameter for the equation of balance of forces, under the assumption of negligible inertial forces. Related to the motions of the body and the surface, we define the displacement fields  $\mathbf{u}(X, t) = f(X, t) - X$ ,  $X \in \mathcal{B}$  and  $\mathbf{u}_s(X, t) = f_s(X, t) - X = \mathbf{u}|_{\mathcal{S}}$ ,  $X \in \mathcal{S}$ .

Let us indicate with  $\mathcal{TB}$  and  $\mathcal{TS}$  the tangent bundles of the body  $\mathcal{B}$  and of the boundary surface  $\mathcal{S}$ , respectively; their current counterparts are denoted with  $\mathcal{TB}_t$  and  $\mathcal{TS}_t$ . By virtue of the Euclidean structure of the space  $\mathcal{E}$  surrounding  $\mathcal{B}$ , the tangent spaces  $\mathcal{T}_X\mathcal{B}$  and  $\mathcal{T}_x\mathcal{B}_t$  can be identified with  $\mathcal{V}$ , while the tangent spaces  $\mathcal{T}_X\mathcal{S}$  and  $\mathcal{T}_x\mathcal{S}_t$  are two-dimensional subspaces of  $\mathcal{V}$ . The tangent bundle  $\mathcal{TS}$  is spanned by the covariant basis field  $\mathbf{a}_\alpha$  and by the contravariant basis field  $\mathbf{a}^\alpha$ , with  $\alpha = 1, 2$ ; the dyadic product between the elements of such bases allows to construct the surface projection tensor<sup>1</sup>  $\mathbf{P} = \mathbf{I} - \mathbf{m} \otimes \mathbf{m} = \mathbf{a}_\alpha \otimes \mathbf{a}^\alpha$ , which projects a vector that belongs to  $\mathcal{V}$  on  $\mathcal{TS}$  (for each  $t \in \mathcal{I}$ ), being  $\mathbf{I}$  the identity of  $\mathcal{V}$ . Here  $\mathbf{m} = \mathbf{a}_1 \times \mathbf{a}_2 / |\mathbf{a}_1 \times \mathbf{a}_2| = \mathbf{a}_3 = \mathbf{a}^3$  is the unit normal to the surface (Figure 1). The transpose of the surface projection is called inclusion and maps vectors from  $\mathcal{TS}$  to  $\mathcal{V}$ , by simply extending their domain of definition. Together with  $\mathbf{m}$ , the vectors  $\mathbf{a}_\alpha$  and  $\mathbf{a}^\alpha$  form the covariant and contravariant bases for  $\mathcal{V}$ . Analogously, we can introduce a projection tensor  $\mathbf{P}_t : \mathcal{V} \times \mathcal{I} \rightarrow \mathcal{TS}_t$ ,  $\mathbf{P}_t = \mathbf{I} - \mathbf{n} \otimes \mathbf{n} = \mathbf{g}_\alpha \otimes \mathbf{g}^\alpha$ , and the associated inclusion tensor  $\mathbf{P}_t^T$ , where  $\mathbf{n}$  is the outward normal to  $\partial\mathcal{B}_t$  and  $\mathbf{g}_\alpha$  ( $\mathbf{g}^\alpha$ ) is a covariant (contravariant) basis of  $\mathcal{TS}_t$ . We will use the symbols  $\mathbf{m}$  and  $\mathbf{n}$  also to denote the unit normals to reference and current area elements, respectively.

The metric properties of the reference and current boundary surfaces are encoded in the reference surface metric tensor  $\mathbf{A} : \mathcal{TS} \times \mathcal{I} \rightarrow \mathcal{TS}$ ,  $\mathbf{A} = \mathbf{a}_\alpha \otimes \mathbf{a}^\alpha$ , and in the current surface metric tensor  $\mathbf{G} : \mathcal{TS}_t \times \mathcal{I} \rightarrow \mathcal{TS}_t$ ,  $\mathbf{G} = \mathbf{g}_\alpha \otimes \mathbf{g}^\alpha$ , respectively, both tensors having the same component representations as the corresponding projection tensors  $\mathbf{P}$  and  $\mathbf{P}_t$ , but different domains of definition.

Now, let us introduce some surface differential operators. Given a curve  $y : \mathcal{U} \subset \mathbb{R} \rightarrow \mathcal{S}$ ,  $\alpha \mapsto x = y(\alpha)$ , we define the surface gradient  $\nabla_s \phi$  of a scalar field  $\phi : \mathcal{S} \times \mathcal{I} \rightarrow \mathbb{R}$  and the surface

---

<sup>1</sup>Unless explicitly specified, summation convention is used, with Latin indices ranging from 1 to 3 and Greek indices ranging from 1 to 2.

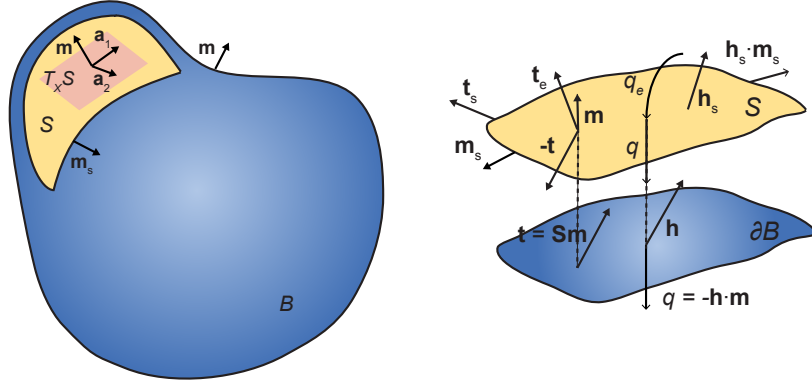


Figure 1: Sketch of the reference configuration of a body with a boundary material surface. The exploded view shows the notation and the directions for the fluxes and the contact forces exchanged by the body and the material surface.

gradient  $\nabla_s \mathbf{v}$  of a superficial vector field  $\mathbf{v} : \mathcal{S} \times \mathcal{I} \rightarrow \mathcal{V}$  through the following chain rules:

$$\left. \frac{d}{d\alpha} \phi(y(\alpha), t) \right|_{\alpha=c} = \nabla_s \phi(x, t) \cdot y'(c), \quad \left. \frac{d}{d\alpha} \mathbf{v}(y(\alpha), t) \right|_{\alpha=c} = \nabla_s \mathbf{v}(x, t)[y'(c)], \quad (1)$$

that is,  $\nabla_s \phi$  and  $\nabla_s \mathbf{v}$  are the operators that, acting on the tangent vector  $y'(c)$  at  $x = y(c)$  to a curve  $y$  belonging to the surface, deliver the rates of change of the fields  $\phi$  and  $\mathbf{v}$  along the curve, respectively, evaluated at the point  $x$  of the curve and at a fixed time  $t$ . A superficial vector field  $\mathbf{v} : \mathcal{S} \times \mathcal{I} \rightarrow \mathcal{TS}$  is called tangential. Then, we define the tangential derivative  $\nabla_{\parallel s} \mathbf{v}$  of a superficial vector field as

$$\nabla_{\parallel s} \mathbf{v} = \mathbf{P} \nabla_s \mathbf{v}, \quad (2)$$

and we take the surface divergence of a vector field as the trace (the inner product with the surface metric) of its tangential derivative:

$$\text{div}_s \mathbf{v} = \text{tr}(\nabla_{\parallel s} \mathbf{v}). \quad (3)$$

The surface divergence of a superficial tensor field  $\mathbf{B} : \mathcal{TS} \times \mathcal{I} \rightarrow \mathcal{V}$  is defined as its analogous operator in  $\mathcal{E}$ , that is, through the identity

$$\text{div}_s \mathbf{B}^T \mathbf{v} = \text{div}_s \mathbf{B} \cdot \mathbf{v}, \quad (4)$$

for all constant vectors  $\mathbf{v} \in \mathcal{V}$ . A frequently used divergence identity that involves a superficial tensor field  $\mathbf{B}$  and a superficial vector field  $\mathbf{v}$  is

$$\text{div}_s \mathbf{B}^T \mathbf{v} = \text{div}_s \mathbf{B} \cdot \mathbf{v} + \mathbf{B} \cdot \nabla_s \mathbf{v}. \quad (5)$$

Further, let us recall the divergence theorem for a superficial vector field  $\mathbf{v}$ :

$$\int_{\partial S} \mathbf{v} \cdot \mathbf{m}_s = \int_S \text{div}_s \hat{\mathbf{v}} \quad (6)$$

where  $\mathbf{m}_s$  is the unit normal to  $\partial S$  and  $\hat{\mathbf{v}} = \mathbf{v} - (\mathbf{v} \cdot \mathbf{m})\mathbf{m}$  the tangential component of  $\mathbf{v}$ . From this result, we can recover the divergence theorem for a superficial tensor field  $\mathbf{B}$ : choosing  $\hat{\mathbf{v}} = \mathbf{B}^T \mathbf{k}$  in (6), with  $\mathbf{k}$  an arbitrary constant vector, and using the definition (4) we get

$$\int_{\partial S} \mathbf{B} \mathbf{m}_s = \int_S \text{div}_s \mathbf{B}. \quad (7)$$

By means of the above definitions of differential operators, we can represent the tangent maps (also called the deformation gradients)  $\mathbf{F} = \nabla f = \mathbf{I} + \nabla \mathbf{u}$  and  $\mathbf{F}_s = \mathbf{P}_t \mathbf{F}|_{\mathcal{S}} \mathbf{P}^T$  that send, respectively, at any time, elements of the tangent bundles  $\mathcal{TB}$  and  $\mathcal{TS}$  to elements of the tangent bundles  $\mathcal{TB}_t$  and  $\mathcal{TS}_t$ . In the following, we will make use of the tensor  $\hat{\mathbf{F}} = \mathbf{P}^T + \nabla_s \mathbf{u}_s = \mathbf{F}|_{\mathcal{S}} \mathbf{P}^T$ , which is the restriction of the domain of the deformation gradient  $\mathbf{F}$  to  $\mathcal{TS} \times \mathcal{I}$ . Note that  $\hat{\mathbf{F}}$  is not invertible;  $\mathbf{F}_s$  is its invertible counterpart. As measures of stretch, we take the right Cauchy-Green tensors  $\mathbf{C} = \mathbf{F}^T \mathbf{F}$  and  $\mathbf{C}_s = \hat{\mathbf{F}}^T \hat{\mathbf{F}} = \mathbf{F}_s^T \mathbf{F}_s$ .

As usual, the determinant  $J = \det \mathbf{F}$  of the deformation gradient measures the local change in volume, while the local area change is computed through the cofactor  $\mathbf{F}^* = J \mathbf{F}^{-T}$  as  $|\mathbf{F}^* \mathbf{m}|$ . Thus, in particular, the ratio  $dS_t/dS$  between the current and the reference area elements of the boundary surface is  $|\mathbf{F}^*|_{\mathcal{S}} \mathbf{m}|$  or it may be alternatively computed by exploiting the geometrical meaning of the cross product between basis vectors as follows:

$$J_s = \frac{dS_t}{dS} = \frac{|\mathbf{F}_s \mathbf{a}_1 \times \mathbf{F}_s \mathbf{a}_2|}{|\mathbf{a}_1 \times \mathbf{a}_2|},$$

with  $J_s = \det \mathbf{F}_s$ . Because solvent absorption locally induces a change in volume of the boundary membrane modeled by the material surface, we attach to  $\mathcal{S}$  a *scalar microstructure*  $\delta(X, t)$ ,  $X \in \mathcal{S}$  that measures the thickness stretch of the membrane, *i.e.* the ratio between the current and the reference thickness  $h(X)$  of the membrane, which contributes to the volume change of the membrane together with the area change of the surface measured by  $J_s$ . We will specify with the relation between swelling and volume change of the membrane in Section 3.3. The kinematics of the boundary material surface  $\mathcal{S}$  is then described by the pair of fields  $(\mathbf{u}_s, \delta)$ .

### 3. Balance equations for a body with a swelling material surface

We consider mechanics and solvent transport as the physics that characterize the behavior of both the body and the boundary membrane. We adopt a referential description for the balance equations; the corresponding spatial description may be derived by applying appropriate push-forward operations. To account for the swelling of the body and of the boundary membrane, we formulate the kinematic constraints that express the volume change induced by the migration of solvent. Hence, we arrive at the formulation of a swelling material surface model. Furthermore, we establish the constitutive equations for the bulk and the swelling material surface through thermodynamical arguments.

#### 3.1. Balance equations for the body

With reference to Lucantonio et al. (2013), we briefly recall the mechanical balance equations and the balance of solvent mass for the body. We consider a system of forces  $(\mathbf{f}, \mathbf{t})$  acting on the body, with  $\mathbf{f}$  the body load per unit reference volume and  $\mathbf{t}$  the boundary load per unit reference area. As usual, the balances of forces and moments for the body read

$$\operatorname{div} \mathbf{S} + \mathbf{f} = \mathbf{0} \quad \text{on } \mathcal{B} \times \mathcal{I}, \quad \mathbf{t} = \mathbf{S} \mathbf{m} \quad \text{on } \partial \mathcal{B} \times \mathcal{I}, \quad \operatorname{skw}(\mathbf{S} \mathbf{F}^T) = \mathbf{0} \quad \text{on } \mathcal{B} \times \mathcal{I}, \quad (8)$$

where  $\mathbf{S}$  is the reference (Piola-Kirchhoff) stress. In particular, on  $\mathcal{S} \subset \partial \mathcal{B}$ ,  $\mathbf{t}$  is the contact force per unit area applied by the membrane to the body.

For solvent transport, upon introducing the solvent concentration field  $c : \mathcal{B} \times \mathcal{I} \rightarrow \mathbb{R}^+$  per unit reference volume and the solvent mass flux  $\mathbf{h} : \mathcal{B} \times \mathcal{I} \rightarrow \mathcal{V}$  per unit reference area, the balance of solvent mass reads

$$\dot{c} = -\operatorname{div} \mathbf{h} \quad \text{on } \mathcal{B} \times \mathcal{I}, \quad -\mathbf{h} \cdot \mathbf{m} = q \quad \text{on } \partial \mathcal{B} \times \mathcal{I}, \quad (9)$$

where  $q$  is the solvent mass boundary source, which corresponds on  $\mathcal{S}$  to the flux from the membrane to the body.

### 3.2. Balance equations for the swelling material surface

In a similar fashion to what we have done for the body, we describe the forces acting on an arbitrary, regular subsurface  $\mathcal{P}_b \subset \mathcal{S}$  by the pair of vector fields  $(\mathbf{f}_s, \mathbf{t}_s)$ , where  $\mathbf{f}_s$  is the force per unit area, which represents the distributed surface load over  $\mathcal{P}_b$ , and  $\mathbf{t}_s$  is the contact force per unit length along  $\partial\mathcal{P}_b$ . The surface load  $\mathbf{f}_s$  consists of the distributed contact forces  $-\mathbf{t}$  exerted by the body on the boundary material surface and of the distributed applied forces  $\mathbf{f}_e$  exerted by the environment on  $\mathcal{S}$ :  $\mathbf{f}_s = \mathbf{f}_e - \mathbf{t}$ . Additionally, we introduce the surface load  $c_n$  that represents the external force per unit area spending power on changes in thickness.

We proceed with deriving the balance equations following the method of virtual power (Germain, 1973). Thus, we prescribe the following version of the principle of virtual power:

$$\int_{\mathcal{P}_b} (\mathbf{S}_s \cdot \nabla_s \tilde{\mathbf{v}}_s + \sigma_n \tilde{\eta}) = \int_{\partial\mathcal{P}_b} \mathbf{t}_s \cdot \tilde{\mathbf{v}}_s + \int_{\mathcal{P}_b} (\mathbf{f}_s \cdot \tilde{\mathbf{v}}_s + c_n \tilde{\eta}) \quad (10)$$

for any  $\mathcal{P}_b \subset \mathcal{S}$  and for any choice of the virtual surface velocity field  $\tilde{\mathbf{v}}_s$  and of the virtual thickness stretch rate  $\tilde{\eta}$ . Here we have introduced the boundary stresses  $\mathbf{S}_s : \mathcal{T}\mathcal{S} \times \mathcal{I} \rightarrow \mathcal{V}$  and  $\sigma_n : \mathcal{S} \times \mathcal{I} \rightarrow \mathbb{R}$  and we are neglecting both applied and contact couples, consistent with the classical theory of membranes (see Remark below). The functional at the right hand side is the external virtual power  $\Pi_{ext}$ , while that at the left hand side is the internal virtual power  $\Pi_{int}$ .

First, by taking  $\tilde{\eta} = 0$  in (10), using the surface divergence theorem (7) and localizing, we obtain the equations of balance of forces for the surface

$$\operatorname{div}_s \mathbf{S}_s + \mathbf{f}_s = \mathbf{0}, \quad \text{on } \mathcal{S} \times \mathcal{I}, \quad (11)$$

$$\mathbf{t}_s = \mathbf{S}_s \mathbf{m}_s, \quad \text{on } \partial\mathcal{S} \times \mathcal{I}. \quad (12)$$

where  $\mathbf{m}_s$  is the unit normal to  $\partial\mathcal{P}_b$ . Then, with  $\tilde{\mathbf{v}}_s = \mathbf{0}$ , from eq. (10) we derive the equations of balance of thickness forces

$$\sigma_n = c_n, \quad \text{on } \mathcal{S} \times \mathcal{I}. \quad (13)$$

To give a physical interpretation to eq. (13), we may picture the microstructure as a distribution of deformable segments attached to the surface, which only resist to stretching; then, eq. (13) represents the force balance along direction parallel to each segment and  $\sigma_n$  plays the role of a thickness stress.

According to the principle of frame-indifference, the internal virtual power (and then, because of the equality, the external virtual power) must be invariant under changes of observer, which implies that  $\Pi_{int}$  must vanish for each rigid virtual surface velocity field of the form

$$\tilde{\mathbf{v}}_s = \tilde{\mathbf{v}}_{so} + \boldsymbol{\omega} \times (x - x_o), \quad \nabla_s \tilde{\mathbf{v}}_s = \mathbf{W} \hat{\mathbf{F}}, \quad (14)$$

with  $x = f(X, t)$ ,  $X \in \mathcal{S}$ ,  $x_o \in \mathcal{E}$ ,  $\tilde{\mathbf{v}}_{so}, \boldsymbol{\omega}$  arbitrary vectors and  $\mathbf{W}$  a skew-symmetric tensor. This condition provides, on localizing,

$$\operatorname{skw}(\hat{\mathbf{F}} \mathbf{S}_s^T) = \mathbf{0}, \quad (15)$$

or, equivalently,  $\mathbf{F}_s \mathbf{S}_s^T \mathbf{P}_t^T = \mathbf{P}_t \mathbf{S}_s \mathbf{F}_s^T$ . Eq. (15) is a restriction on the constitutive prescriptions for  $\mathbf{S}_s$  and implies that the surface does not carry internal forces along the normal direction to its deformed shape:  $\mathbf{S}_s \mathbf{a}^\alpha \cdot \mathbf{n} = 0$ . Indeed,  $\operatorname{skw}(\hat{\mathbf{F}} \mathbf{S}_s^T) \mathbf{v} = \mathbf{S}_s \mathbf{a}^\alpha \times \mathbf{g}_\alpha \times \mathbf{v}$ ,  $\forall \mathbf{v} \in \mathcal{V}$  (no sum on  $\alpha$ ).

As concerns surface solvent transport, we introduce the referential boundary solvent concentration field  $c_s : \mathcal{S} \times \mathcal{I} \rightarrow \mathbb{R}^+$ , which measures the number of solvent moles per unit area of  $\mathcal{S}$ . The boundary surface can exchange solvent pointwise in  $\mathcal{S}$  with the bulk  $\mathcal{B}$ , and through its

boundary  $\partial\mathcal{S}$  with the environment. Then, the balance of solvent mass for an arbitrary, regular subsurface  $\mathcal{P}_b \subset \mathcal{S}$  of the material boundary reads

$$\frac{d}{dt} \int_{\mathcal{P}_b} c_s = - \int_{\partial\mathcal{P}_b} \mathbf{h}_s \cdot \mathbf{m}_s + \int_{\mathcal{P}_b} q_s, \quad (16)$$

where  $\mathbf{m}_s$  is the outward unit normal to  $\partial\mathcal{S}$ ,  $\mathbf{h}_s : \mathcal{S} \times \mathcal{I} \rightarrow \mathcal{TS}$  is the boundary solvent flux and the solvent mass boundary source  $q_s = -q + q_e$  includes the exchange of solvent with the bulk and the external supply  $q_e$  of solvent. Using the surface divergence theorem (6) for a vector field (with  $\mathbf{h}_s \cdot \mathbf{m} = 0$ , since  $\mathbf{h}_s$  is a tangential vector field), eq. (16) localizes to

$$\dot{c}_s = -\operatorname{div}_s \mathbf{h}_s + q_s, \quad \text{on } \mathcal{S} \times \mathcal{I}. \quad (17)$$

*Remark.* Equations (11) and (15) are the mechanical balance equations for a membrane, *i.e.* a thin shell-like body with negligible bending stiffness, which can only carry internal forces tangent to its deformed shape. Those equations may also be recovered from the balance equations for a special Cosserat shell (Antman, 2005), where the director  $l$  is constrained to be a unit vector (the thickness does not change), by imposing that both the contact couples, represented<sup>2</sup> by the couple tensor  $M$ , and the applied body couples  $c \times l$  and boundary couples  $m \times l$  are zero. For shells with thickness distension (DiCarlo et al., 2001), the balance of director forces adds to the governing equations:

$$(\operatorname{div}_s M - Ne + c) \cdot l = 0, \quad \text{on } \mathcal{S}, \quad (18)$$

$$M\nu \cdot l = m \cdot l, \quad \text{on } \partial\mathcal{S}; \quad (19)$$

where  $\nu$  is the unit normal to  $\partial\mathcal{S}$ . Then, eq. (18) reduces to eq. (13) under the hypotheses  $M = 0$  and  $m \cdot l = 0$ , and by recognizing that  $\sigma_n$  corresponds to the component  $Ne \cdot l$  along the director  $l$  of the contact force per unit length  $Ne$  exchanged between parts of the shell through cut-planes that are orthogonal to the reference director  $e$ , and  $c_n$  corresponds to the director bulk-force  $c \cdot l$ . In turn, the balance equations for a shell, including the balance of director forces, may be derived from the principle of virtual power for a three-dimensional Cauchy continuum, by employing the appropriate representations for both the true and the virtual displacement fields. Such a deductive approach allows to extend the present model by considering a richer kinematics and to derive a hierarchy of structural theories having different degrees of approximation from three-dimensional continuum mechanics. Here, however, we prefer a direct approach, which we find rather straightforward, since it avoids the introduction of additional structure (*i.e.* the director) that is redundant for a model of material surface with a scalar microstructure.

### 3.3. Swelling constraints

Up to this point, we have introduced the balance equations that allow for the description of coupled elasticity and solvent transport phenomena in boundary material surfaces. Henceforth, we specialize the theory for swelling materials, with specific reference to polymer gels, which are mixtures of an elastomeric matrix and a solvent, where the change in solvent content causes a change in volume (swelling) of the aggregate. Because gels often possess a certain amount of solvent in their preparation state, it is convenient to measure the volume change starting from a swollen configuration, where the solvent concentration is homogeneous and equal to  $c_o$  in the bulk, and to  $c_{so}$  on the surface. The swollen reference configurations  $\mathcal{B}$  and  $\mathcal{S}$  are conceived

---

<sup>2</sup>Here we use the same notation as in (DiCarlo et al., 2001).

as being reached from the corresponding dry states through the homogeneous and isotropic deformations, characterized by the stretches  $\lambda_o$  and  $\lambda_{so}$ , respectively. Moreover, we specify that  $\mathcal{B}$  and  $\mathcal{S}$  are stress-free configurations and that both the body and the surface are in chemical equilibrium with an external solvent. We will see in Section 4 how to characterize  $\mathcal{B}$  and  $\mathcal{S}$  from the thermodynamical equilibrium viewpoint.

Usually, the solvent is liquid and together with the elastomeric matrix they are assumed to be incompressible, so that the local volume ratio  $J$  from  $\mathcal{B}$  relates to the change in solvent concentration as (Lucantonio et al., 2013):

$$J = 1 + \Omega(c - c_o), \quad (20)$$

where  $\Omega$  is the solvent molar volume.

For a boundary membrane that consists of a swelling material, we may formulate an analogous constraint for  $\mathcal{S}$ . As noted in the introduction, for this purpose, the boundary surface  $\mathcal{S}$  is considered as the base surface of the three-dimensional membrane; thus, the swelling constraint involves both the area change of  $\mathcal{S}$  and the thickness change  $\delta$  of the membrane. If we approximate the solvent concentration  $c$  in the membrane with its value  $c|_{\mathcal{S}}$  on  $\mathcal{S}$ , the solvent volume contained in an infinitesimal reference volume of the membrane  $dV = h dS$  is  $\Omega c|_{\mathcal{S}} dV = \Omega c_s dS$ . Hence, the infinitesimal current volume, whose change is determined by the change in solvent content, is  $dV(1 + \Omega(c|_{\mathcal{S}} - c_o|_{\mathcal{S}})) = dV(1 + \Omega(c_s - c_{so})/h)$  and we can express the local volume ratio  $J$  for the membrane as

$$J = 1 + \Omega(c|_{\mathcal{S}} - c_o|_{\mathcal{S}}) = 1 + \frac{\Omega}{h}(c_s - c_{so}), \quad (21)$$

where  $c_{so} = h c_o|_{\mathcal{S}} = (\lambda_{so}^3 - 1)h/(\Omega \lambda_{so}^3)$  is the initial solvent concentration in the reference state. Upon introducing the equivalent molar volume  $\Omega_s = \Omega/h$  and by employing the following representation for the deformation gradient of the membrane:

$$\mathbf{F} \approx \mathbf{F}|_{\mathcal{S}} = \hat{\mathbf{F}}\mathbf{P} + \delta \mathbf{n} \otimes \mathbf{m} \quad (22)$$

so that  $J \approx J|_{\mathcal{S}} = \delta J_s$ , the counterpart of the swelling constraint (20) for the membrane reads

$$\delta J_s = \delta(\det \mathbf{C}_s)^{1/2} = 1 + \Omega_s(c_s - c_{so}). \quad (23)$$

Notice that, by taking the time derivative of eq. (23) and replacing  $\dot{c}_s$  with eq. (17), we obtain an evolution equation for the thickness stretch:

$$\dot{\delta} J_s + \delta \dot{J}_s + \Omega_s(\operatorname{div}_s \mathbf{h}_s - q_s) = 0. \quad (24)$$

*Remark.* The thickness stretch  $\delta$  may be used as a primary variable of the formulation, instead of the boundary concentration  $c_s$  – and then, (24) replaces (17) as the equation of balance of solvent mass for the surface – by systematically using the volume constraint (23) to eliminate  $c_s$  in the governing equations of the problem, including the constitutive equations (see Section 4).

### 3.4. Continuity conditions

We recall that the displacement field is continuous  $\mathbf{u}_s = \mathbf{u}|_{\mathcal{S}}$  because of the continuity of the motion  $f$  up to  $\partial\mathcal{B}$ , since we are assuming that the boundary surface is always bonded to the body. In addition, we assume that the boundary material surface is in chemical equilibrium with the adjacent layer of material that belongs to the body. Hence, at any time, the chemical potential is continuous at  $\mathcal{S}$ :

$$\mu_s = \mu|_{\mathcal{S}}. \quad (25)$$

This constraint determines (implicitly) the solvent flux  $q$  exchanged between the surface and the body and will be enforced in the numerical model through a Lagrange multiplier.



*Remark.* In (McBride et al., 2011) it is shown that the chemical continuity condition (25) need not be assumed from the onset, but it is rather one of the possible ways to satisfy the dissipation inequality (see Section 4).

#### 4. Thermodynamics and constitutive equations

With reference to (Lucantonio et al., 2013), we assume that the bulk material is allowed to exchange mechanical power and power due to solvent transport with the exterior. Thermodynamical arguments based on the Coleman–Noll procedure lead, in an isothermal setting, to the following constitutive restrictions:

$$\mathbf{S} = \frac{\partial \psi}{\partial \mathbf{F}} - p \mathbf{F}^*, \quad \mu = \frac{\partial \psi}{\partial c} + \Omega p, \quad \mathbf{h} \cdot \nabla \mu \leq 0, \quad (26)$$

where  $\psi$  is the Helmholtz free energy per unit volume in  $\mathcal{B}$ ,  $\mu$  is the bulk solvent chemical potential and  $p$  is the bulk solvent pressure. For polymer gels, the Flory–Rehner free energy is commonly employed as a representation form for  $\psi$ :

$$\psi(\mathbf{F}, c) = \frac{1}{2} \frac{G}{J_o} (\lambda_o^2 \mathbf{F} \cdot \mathbf{F} - 3) + \frac{1}{J_o} \frac{\mathcal{R}T}{\Omega} \left[ \Omega J_o c \log \left( \frac{\Omega J_o c}{1 + \Omega J_o c} \right) + \chi \frac{\Omega J_o c}{1 + \Omega J_o c} \right], \quad (27)$$

where  $G$  is the shear modulus of the dry polymer,  $J_o = \lambda_o^3$  is the initial swelling ratio,  $\mathcal{R}$  is the universal gas constant,  $T$  is the absolute temperature and  $\chi$  is the dimensionless measure of the solvent–polymer enthalpy of mixing. The first term in (27) represents the change in free energy due to the deformation of the polymer network, while the second term is the contribution to the free energy due to the mixing between the solvent and the polymer network. Further, we choose the following representation for the solvent flux

$$\mathbf{h} = -\frac{cD}{\mathcal{R}T} \nabla \mu \quad (28)$$

which refers to a mobility tensor  $\mathbf{D} = (cD/\mathcal{R}T)\mathbf{I}$  that varies linearly with the volume change and is isotropic with respect to the reference configuration (referential isotropy assumption). A discussion of the effects of the spatial isotropy assumption, as compared to the referential isotropy assumption, can be found in (Lucantonio et al., 2013), together with the representation of  $\mathbf{M}$  for a transversely-isotropic material.

We then proceed with formulating the thermodynamics for the boundary material surface. In an isothermal setting, the free energy imbalance requires that the time-rate of the free energy for a part  $\mathcal{P}_b \subset \mathcal{S}$  be less or equal to the sum of the mechanical power  $\mathcal{W}$  and to the power  $\Upsilon$  associated to solvent transport:

$$\frac{d}{dt} \int_{\mathcal{P}_b} \psi_s \leq \mathcal{W} + \Upsilon, \quad (29)$$

where  $\psi_s$  is the surface Helmholtz free energy per unit reference area. With the following representations for the external powers

$$\mathcal{W} = \int_{\mathcal{P}_b} \mathbf{f}_s \cdot \dot{\mathbf{u}}_s + \int_{\partial \mathcal{P}_b} \mathbf{t}_s \cdot \dot{\mathbf{u}}_s + \int_{\mathcal{P}_b} c_n \dot{\delta}, \quad \Upsilon = - \int_{\partial \mathcal{P}_b} \mu_s \mathbf{h}_s \cdot \mathbf{m}_s + \int_{\mathcal{P}_b} \mu_s q_s, \quad (30)$$

the free energy imbalance for  $\mathcal{P}_b$  reads

$$\begin{aligned} \frac{d}{dt} \int_{\mathcal{P}_b} \psi_s - \int_{\mathcal{P}_b} p_s (\dot{\delta} J_s + \delta \dot{J}_s - \Omega_s \dot{c}_s) \leq & \int_{\mathcal{P}_b} \mathbf{f}_s \cdot \dot{\mathbf{u}}_s + \int_{\partial \mathcal{P}_b} \mathbf{t}_s \cdot \dot{\mathbf{u}}_s + \\ & + \int_{\mathcal{P}_b} c_n \dot{\delta} - \int_{\partial \mathcal{P}_b} \mu_s \mathbf{h}_s \cdot \mathbf{m}_s + \int_{\mathcal{P}_b} \mu_s q_s, \end{aligned} \quad (31)$$

where the swelling constraint (23) has been enforced through the Lagrange multiplier  $p_s$ , which represents the surface solvent pressure. Using the divergence theorem (6), the balance equations (11)-(13) and (17), the identity (5) and the continuity condition (25) we find the localized version of the free energy imbalance

$$\dot{\psi}_b \leq \mathbf{S}_s^c \cdot \hat{\mathbf{F}} + \sigma_n^c \dot{\delta} + \mu_s^c \dot{c}_s - \mathbf{h}_s \cdot \nabla_s \mu_s, \quad (32)$$

where  $\mathbf{S}_s^c = \mathbf{S}_s + p_s \delta \mathbf{P}_t^T \mathbf{F}_s^*$ ,  $\sigma_n^c = \sigma_n + p_s J_s$  and  $\mu_s^c = \mu_s - p_s \Omega_s$  are the constitutively determinate parts of the reference boundary stress, of the normal stress and of the boundary chemical potential. Inequality (32) suggests that the constitutive functions that deliver  $\psi_s$ ,  $\mathbf{S}_s^c$ ,  $\sigma_n^c$ ,  $\mu_s^c$  and  $\mathbf{h}_s$  have to be prescribed. In particular, we assume that all these functions depend on  $(\hat{\mathbf{F}}, \delta, c_s)$ , while  $\mathbf{h}_s$  also depends on  $\nabla_s \mu_s$ . By requiring that (32) be satisfied for every admissible constitutive process, we obtain the following thermodynamic restrictions

$$\mathbf{S}_s = \frac{\partial \psi_s}{\partial \hat{\mathbf{F}}} - p_s \delta \mathbf{P}_t^T \mathbf{F}_s^*, \quad \sigma_n = \frac{\partial \psi_s}{\partial \delta} - p_s J_s, \quad (33)$$

$$\mu_s = \frac{\partial \psi_s}{\partial c_s} + p_s \Omega_s, \quad \mathbf{h}_s(\hat{\mathbf{F}}, c_s, \nabla_s \mu_s) \cdot \nabla_s \mu_s \leq 0. \quad (34)$$

Substitution of (33)<sub>2</sub> into the local form of the balance equation (13) allows to obtain an expression for the pressure  $p_s$ :

$$p_s = \frac{1}{J_s} \left( \frac{\partial \psi_s}{\partial \delta} - c_n \right), \quad (35)$$

which can be used to eliminate the pressure from the governing equations of the model. Also notice that the microstructure  $\delta$  can be eliminated too from the formulation, through eq. (23), and it is thus called a *latent microstructure* (Capriz, 1989). Hence, we are left with  $\mathbf{u}_s$  and  $c_s$  as the primary unknowns of the governing equations for the boundary surface.

In analogy with eq. (28), we satisfy the requirement (34)<sub>2</sub> by choosing the following constitutive law:

$$\mathbf{h}_s = -\frac{c_s D_s}{\mathcal{R}T} \nabla_s \mu_s, \quad (36)$$

where  $D_s$  is the diffusivity of the solvent within the boundary membrane.

*Remark.* Without the continuity condition (25), the last term in (31) should be replaced by two contributions:

$$\int_{\mathcal{P}_b} \mu_s q_e - \int_{\mathcal{P}_b} \mu|_S q \quad (37)$$

where we have distinguished between the chemical potential  $\mu|_S$  associated to the flux  $q$ , and the chemical potential  $\mu_s$  associated to the boundary source  $q_e$ . Then, the free energy imbalance (32) becomes

$$\dot{\psi}_b \leq \mathbf{S}_s^c \cdot \hat{\mathbf{F}} + \sigma_n^c \dot{\delta} + \mu_s^c \dot{c}_s - \mathbf{h}_s \cdot \nabla_s \mu_s + (\mu|_S - \mu_s) \mathbf{h}|_S \cdot \mathbf{m}; \quad (38)$$

with the constitutive restrictions (33)-(34)<sub>1</sub> and (36), we obtain the reduced free energy imbalance

$$(\mu|_S - \mu_s)\mathbf{h}|_S \cdot \mathbf{m} \geq 0 \quad (39)$$

which may be satisfied, for instance, by imposing a Robin-like constraint between the jump of the chemical potential at the surface and the solvent flux exchanged with the bulk:

$$(\mu|_S - \mu_s) = k(\mathbf{h}|_S \cdot \mathbf{m}), \quad k \geq 0. \quad (40)$$

A similar discussion can be found in (McBride et al., 2011).

#### 4.1. A surface free energy for polymer gels

In this section we focus on the derivation of a surface energy density for a membrane made of a polymer gel, whose dry shear modulus is  $G_s$  and whose solvent-polymer interaction parameter is  $\chi_s$ . For such swelling boundary membrane we take as a representation form for the free energy eq. (27), *i.e.* the same form as for the body, with  $G$  replaced by  $G_s$ ,  $\lambda_o$  by  $\lambda_{so}$ ,  $J_o$  by  $J_{so} = \lambda_{so}^3$  and  $\chi$  by  $\chi_s$ . To reduce the free energy (27) to a surface energy density, we consider again the representation (22) for deformation gradient of the membrane, which accounts for both the change of metric properties of the surface and the change in thickness, and the approximation  $c \approx c|_S$  for the concentration field, as done in Section 3.3. The kinematic hypotheses for  $\mathbf{F}$  and  $c$  are limited, as in (Libai and Simmonds, 1998), to the derivation of the surface free energy and thus leave unchanged the balance equations for the surface. Then, by integrating (27) over the thickness, we get:

$$\psi_s(\hat{\mathbf{F}}, c_s) = \int_0^h \psi(\mathbf{F}, c) = \frac{1}{2} \frac{G_s}{J_{so}} h (\lambda_{so}^2 \text{tr}(\mathbf{C}_s) + \lambda_{so}^2 \delta^2 - 3) + \frac{1}{J_{so}} \frac{\mathcal{R}T}{\Omega_s} g(c_s), \quad (41)$$

with

$$g(c_s) = \Omega_s J_{so} c_s \log \left( \frac{\Omega_s J_{so} c_s}{1 + \Omega_s J_{so} c_s} \right) + \chi_s \frac{\Omega_s J_{so} c_s}{1 + \Omega_s J_{so} c_s}, \quad (42)$$

so that eqs. (33)-(34) and (35) yield

$$\mathbf{S}_s = \frac{G_s}{\lambda_{so}} h \hat{\mathbf{F}} - p_s \delta \mathbf{P}_t^T \mathbf{F}_s^* = \frac{G_s}{\lambda_{so}} h \hat{\mathbf{F}} - p_s \frac{\delta}{J_s} \hat{\mathbf{F}} \mathbf{C}_s^*, \quad (43)$$

$$p_s = \frac{G_s}{\lambda_{so}} h \frac{\delta}{J_s} - \frac{c_n}{J_s}, \quad (44)$$

$$\mu_s = \mathcal{R}T \left[ \log \frac{\Omega_s J_{so} c_s}{1 + \Omega_s J_{so} c_s} + \frac{1}{1 + \Omega_s J_{so} c_s} + \frac{\chi_s}{(1 + \Omega_s J_{so} c_s)^2} \right] + \Omega_s p_s. \quad (45)$$

*Free swelling equilibrium.* The free swelling equilibrium is attained when the system is allowed to swell without any applied loads ( $\mathbf{t} = \mathbf{t}_s = \mathbf{f} = \mathbf{f}_e = \mathbf{0}$ ,  $c_n = 0$ ) or mechanical constraints and to attain chemical equilibrium with an external solvent at a fixed, homogeneous chemical potential  $\mu_e$ . The chemo-mechanical equilibrium is characterized by the conditions of zero stress and homogeneous chemical potential:

$$\mathbf{S} = \mathbf{0}, \quad \mathbf{S}_s = \mathbf{0}, \quad \sigma_n = 0, \quad \mu = \mu_s = \mu_e, \quad (46)$$

so that, from the constitutive equations (26) and (43)-(44), it results that the deformation gradient is isotropic and homogeneous, for both the body and the surface<sup>3</sup>

$$\mathbf{F} = \lambda \mathbf{I}, \quad \mathbf{F}_s = \lambda_s \mathbf{g}_\alpha \otimes \mathbf{a}^\alpha, \quad \delta = \lambda_s; \quad (47)$$

---

<sup>3</sup>Here we assume that  $\mathbf{g}_\alpha$  and  $\mathbf{a}^\alpha$  are physical bases.

the concentration fields, from (20) and (21), are readily computed as

$$c = c_o + \frac{\lambda^3 - 1}{\Omega}, \quad c_s = c_{so} + \frac{\lambda_s^3 - 1}{\Omega_s}, \quad (48)$$

and the pressure fields are

$$p = \frac{G}{\lambda_o \lambda}, \quad p_s = \frac{G_s}{\lambda_{so}} \frac{h}{\lambda_s}, \quad (49)$$

while the conditions  $(46)_2$  and the constitutive equations (28) and (36) imply that the solvent flux is zero:  $\mathbf{h} = \mathbf{0}$ ,  $\mathbf{h}_s = \mathbf{0}$ .

By substituting expressions (48) and (49) in  $(26)_2$  and (45) we obtain a set of non-linear algebraic equations determining the chemo-mechanical equilibrium for the body and the surface:

$$\log \frac{(\lambda_s \lambda_{so})^3 - 1}{(\lambda_s \lambda_{so})^3} + \frac{1}{(\lambda_s \lambda_{so})^3} + \frac{\chi_s}{(\lambda_s \lambda_{so})^6} + \frac{G_s \Omega_s}{\mathcal{R}T} \frac{h}{\lambda_s \lambda_{so}} = \frac{\mu_e}{\mathcal{R}T}, \quad (50)$$

$$\log \frac{(\lambda \lambda_o)^3 - 1}{(\lambda \lambda_o)^3} + \frac{1}{(\lambda \lambda_o)^3} + \frac{\chi}{(\lambda \lambda_o)^6} + \frac{G \Omega}{\mathcal{R}T} \frac{1}{\lambda \lambda_o} = \frac{\mu_e}{\mathcal{R}T}, \quad (51)$$

which may be solved for the free swelling stretches  $\lambda$  and  $\lambda_s$ .

For  $\lambda = \lambda_s = 1$ , we derive the equilibrium conditions that characterize the reference configurations  $\mathcal{B}$  and  $\mathcal{S}$ , and define the relations between the dimensionless chemical potential  $\mu_e/\mathcal{R}T$  of the external solvent and the initial swelling stretches  $\lambda_o$  and  $\lambda_{so}$ , depending on the dimensionless parameters  $G\Omega/\mathcal{R}T$ ,  $G_s\Omega_s/\mathcal{R}T$ ,  $\chi$  and  $\chi_s$ .

Notice that, when the body and the surface are made of the same material ( $G = G_s$ ,  $\chi = \chi_s$ , which implies  $\lambda_o = \lambda_{so}$ ), the two equations coincide and the solution is  $\lambda = \lambda_s$ .

## 5. Boundary conditions and weak form of the governing equations

As regards the mechanical boundary conditions, either the boundary loads  $\mathbf{t}$  and  $\mathbf{t}_s$  may be assigned on the portions  $\partial_t \mathcal{B}$  and  $\partial_t \mathcal{S}$  of  $\partial \mathcal{B} \setminus \mathcal{S}$  and  $\partial \mathcal{S}$ , respectively, or the displacements  $\mathbf{u}$  and  $\mathbf{u}_s$  on  $\partial_{\mathbf{u}} \mathcal{B}$  and  $\partial_{\mathbf{u}} \mathcal{S}$ . For solvent transport, the boundary sources  $-\mathbf{h} \cdot \mathbf{m} = q$  or  $-\mathbf{h}_s \cdot \mathbf{m}_s$  may be prescribed on  $\partial_q \mathcal{B} \subset \partial \mathcal{B} \setminus \mathcal{S}$  or  $\partial_q \mathcal{S} \subset \partial \mathcal{S}$ , respectively; alternatively, the chemical potential  $\mu$  or  $\mu_s$  may be prescribed on  $\partial_\mu \mathcal{B} \subset \partial \mathcal{B} \setminus \mathcal{S}$  or  $\partial_\mu \mathcal{S} \subset \partial \mathcal{S}$ , respectively. The latter boundary condition corresponds to the assumption of instantaneous chemical equilibrium of the gel with the external solvent and it can be considered as an implicit Dirichlet boundary condition for the solvent concentration  $c$  or  $c_s$ . Indeed, we may solve the non-linear algebraic equations  $\mu = \mu_e$  or  $\mu_s = \mu_e$ , where  $\mu$  and  $\mu_s$  are given by  $(26)_2$  and (45), written in weak form

$$\int_{\partial_\mu \mathcal{B}} (\mu(\bar{c}, p) - \mu_e) \tilde{c} = 0, \quad \int_{\partial_\mu \mathcal{S}} (\mu_s(\bar{c}_s, p_s) - \mu_e) \tilde{c}_s = 0, \quad (52)$$

for the auxiliary unknowns  $\bar{c}$  and  $\bar{c}_s$  and prescribe the solutions as essential boundary conditions for  $c$  and  $c_s$ :  $c = \bar{c}$  on  $\partial_\mu \mathcal{B}$  and  $c_s = \bar{c}_s$  on  $\partial_\mu \mathcal{S}$ . An analogous approach is used to impose the pointwise chemical equilibrium of the surface  $\mathcal{S}$  with the external solvent in weak form.

We now summarize all the governing equations presented so far, recast in weak form, where

$(\tilde{\mathbf{u}}, \tilde{p}, \tilde{\mu}, \tilde{\mu}_s, \tilde{g})$  denote the test fields corresponding to the unknowns  $(\mathbf{u}, p, c, c_s, g)$  of the problem:

$$-\int_{\mathcal{B}} \mathbf{S} \cdot \nabla \tilde{\mathbf{u}} - \int_{\mathcal{S}} \mathbf{S}_s \cdot \nabla_s \tilde{\mathbf{u}} + \int_{\partial_t \mathcal{B}} \mathbf{t} \cdot \tilde{\mathbf{u}} + \int_{\mathcal{S}} \mathbf{f}_e \cdot \tilde{\mathbf{u}} + \int_{\partial_t \mathcal{S}} \mathbf{t}_s \cdot \tilde{\mathbf{u}} = 0, \quad (53)$$

$$-\int_{\mathcal{B}} [J - 1 - \Omega(c - c_o)] \tilde{p} = 0, \quad (54)$$

$$-\int_{\mathcal{B}} (\dot{c} \tilde{\mu} + \mathbf{h} \cdot \nabla \tilde{\mu}) + \int_{\partial_q \mathcal{B}} q \tilde{\mu} + \int_{\mathcal{S}} g \tilde{\mu} = 0, \quad (55)$$

$$-\int_{\mathcal{S}} [(\dot{c}_s + g - q_e) \tilde{\mu}_s + \mathbf{h}_s \cdot \nabla_s \tilde{\mu}_s] - \int_{\partial_q \mathcal{S}} (\mathbf{h}_s \cdot \mathbf{m}_s) \tilde{\mu}_s = 0, \quad (56)$$

with the solvent flux  $g = \mathbf{h}|_{\mathcal{S}} \cdot \mathbf{m}$  determined by the continuity condition on the chemical potential, which, in weak form, reads

$$\int_{\mathcal{S}} (\mu - \mu_s) \tilde{g} = 0. \quad (57)$$

In writing equation (53), we have expressed the traction  $\mathbf{t}$  on  $\mathcal{S}$  as  $\mathbf{t} = \mathbf{f}_e - \mathbf{f}_s = \mathbf{f}_e + \text{div}_s \mathbf{S}_s$  by (11) and we have used the continuity of the displacement up to  $\mathcal{S}$ . As initial conditions we prescribe:

$$\mathbf{u} = \mathbf{0}, \quad \text{on } \mathcal{B}, \quad \mathbf{u}_s = \mathbf{0}, \quad \text{on } \mathcal{S}, \quad (58)$$

$$p = \frac{G}{\lambda_o}, \quad \text{on } \mathcal{B}, \quad g = 0, \quad \text{on } \mathcal{S}, \quad (59)$$

$$c = c_o, \quad \text{on } \mathcal{B}, \quad c_s = c_{so}, \quad \text{on } \mathcal{S}, \quad (60)$$

where the initial pressure  $p$  is computed from (49) with  $\lambda = 1$  and  $c_o = (\lambda_o^3 - 1)/(\Omega \lambda_o^3)$  and  $c_{so} = (\lambda_{so}^3 - 1)/(\Omega_s \lambda_{so}^3)$  are defined by the initial swelling stretches  $\lambda_o$  and  $\lambda_{so}$ .

We choose the same test functions for  $c$  and  $c_s$  so that, by summing (55) and (56) with  $\tilde{\mu} = \tilde{\mu}_s$ , we recover the weak form of the balance of solvent mass for the system body + material surface:

$$-\int_{\mathcal{B}} (\dot{c} \tilde{\mu} + \mathbf{h} \cdot \nabla \tilde{\mu}) + \int_{\partial_q \mathcal{B}} q \tilde{\mu} - \int_{\mathcal{S}} [(\dot{c}_s - q_e) \tilde{\mu} + \mathbf{h}_s \cdot \nabla_s \tilde{\mu}] - \int_{\partial_q \mathcal{S}} (\mathbf{h}_s \cdot \mathbf{m}_s) \tilde{\mu} = 0. \quad (61)$$

The weak form equations (53)-(57), together with the constitutive equations (26)-(28), (36), and (43)-(45), the swelling constraint (23), and the boundary conditions specified in the following examples, are implemented in the software COMSOL Multiphysics v4.4 and solved using the finite element method.

## 6. Applications

We present several numerical examples to demonstrate the applicability of the model to the study of biomedical devices, soft crawler robots and surface transport phenomena.

### 6.1. Drug release from a hydrogel disk

Certain polymers, such as NIPAAm and its copolymers, exhibit a dramatic de-swelling when temperature is increased beyond a threshold. Based on these polymers, temperature-responsive hydrogels have been produced and investigated as drug delivery systems, where temperature acts

as an external stimulus that modulates the drug release rate. For instance, Bae and coworkers (Bae et al., 1991) fabricated drug-loaded disks made of PNIPAAm-PTMEG interpenetrating polymer networks, which realize an on-off, pulsated drug release. In particular, upon increasing the temperature from 298 K to 303 K, there was a shrinkage of the outer membrane leading to a surface layer with very low permeability to the drug that blocked further drug release.

Inspired by this experiment, we consider a hydrogel disk where, for simplicity, only the coating consists of a thermo-responsive hydrogel. As in the experiment, the disk has a diameter of 10 mm and a thickness of 1 mm. Since the boundary membrane is very thin (thickness  $h = 1 \mu\text{m}$ ), we neglect heat exchange and assume that thermal equilibrium is reached instantaneously, when the temperature is changed. For the initial condition, we assume that the hydrogel disk is fully swollen, in equilibrium with pure water outside ( $\mu_e = 0 \text{ J/mol}$ ), and that mainly water contributes to swelling the hydrogel, while we neglect the contribution of the drug. The disk is constraint-free and its boundary is traction-free; bulk forces are absent.

In the framework of the Flory-Rehner swelling theory, thermo-responsive hydrogels are modeled by prescribing a dependence on the temperature of the mixing affinity between the polymer and the solvent, represented by the dimensionless parameter  $\chi$ . In particular, following (Chester and Anand, 2011), the temperature dependence of the solvent-polymer interaction parameter  $\chi_s$  for the coating layer is taken as

$$\chi_s(T) = \frac{1}{2}(\chi_L + \chi_H) - \frac{1}{2}(\chi_L - \chi_H) \tanh\left(\frac{T - T_t}{\Delta T}\right) \quad (62)$$

where  $T_t$  is the transition temperature,  $\chi_L$  ( $\chi_H$ ) is the value of  $\chi_s$  below (above) the transition temperature, and  $\Delta T$  is the change in temperature in the transition from  $\chi_L$  to  $\chi_H$ .

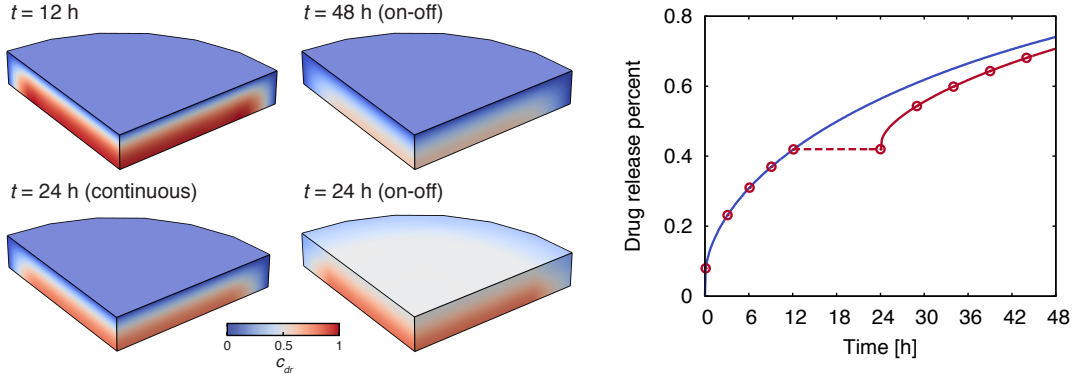


Figure 2: Drug release from a hydrogel disk coated with a thermo-responsive gel. When the temperature is increased beyond the transition temperature, the coating gel shrinks, causing a reduction of the permeability of the surface, which hampers further drug release. (Left) Contour plots of the normalized drug concentration  $c_{dr}$  over  $1/8$  of the hydrogel disk at several times, for the continuous and the on-off release modes. (Right) Percent of drug released from the disk as a function of time, for the continuous release (blue solid line) and for the on-off release (off = dashed line, on = red solid line with circles).

As usual in diffusion-controlled drug delivery systems, where drug diffusion is the rate-limiting process, the transport of the drug within the hydrogel is described by the equation (Siepmann and Siepmann, 2012)

$$\dot{c}_{dr} = D_{dr} \Delta c_{dr} \quad (63)$$

Table 1: Parameter values used in the numerical simulations of the drug delivery system.

Parameter	Value
$\Omega$	$6 \times 10^{-5} \text{ m}^3/\text{mol}$
$D$	$1 \times 10^{-9} \text{ m}^2/\text{s}$
$D_s$	$D$
$D_d$	$2 \times 10^{-12} \text{ m}^2/\text{s}$
$k$	$D_d/h$
$G$	10 kPa
$G_b$	10 kPa (PNIPAAm)
$\chi$	0.2
$\chi_H$	0.6
$\chi_L$	0.2
$T_t$	301 K
$\Delta T$	0.5 K
$T$	298 K (on), 303 K (off)
$\lambda_o$	1.5
$\lambda_{so}$	1.5

where  $c_{dr}$  is a normalized drug concentration, which is initially homogeneous and equal to 1, and  $D_{dr}$  is the drug diffusivity coefficient within the hydrogel. When the membrane is swollen, its permeability increases because the mesh size of the polymer network increases, thus allowing for a higher flow of solvent through it. To model the swelling-dependent permeability of the membrane, we describe the drug flux through the membrane as

$$h_{dr} = -D_{dr} \nabla c_{dr} \cdot \mathbf{m} = -k(J_s \delta)^n (c_{dr}|_S - c_{ext}) \quad (64)$$

where  $k$  is the permeability of the membrane to the drug when  $J_s \delta = 1$ , and  $c_{ext} = 0$  the (dimensionless) drug concentration in the external medium (assuming perfect sink conditions). In the following simulations we set  $n = 10$ .

We performed transient numerical simulations of two drug release profiles:

- continuous drug release: the temperature  $T$  of the medium is held fixed at 298 K, below  $T_t$ ;
- on-off drug release: the temperature  $T$  is held fixed at 298 K for 12 hours, then it is instantaneously increased to  $T = 303 \text{ K} > T_t$  for 12 hours, and then it is decreased back to  $T = 298 \text{ K}$ .

The values for the parameters used in the numerical simulations are reported in Table 1. During the simulations, we monitored the percent of drug released in the medium  $\int_{\mathcal{B}} (1 - c_{dr})/V$  where  $V$  is the volume of the hydrogel disk. In the first case, the drug diffuses continuously out of the disk, while in the second, when the temperature is increased beyond the transition temperature, the coating gel shrinks, causing a reduction of the permeability of the surface, which hampers further drug release (Figure 2). During the off drug release period, the drug concentration in the hydrogel tends to equalize, so that  $c_{dr}$  at the boundary increases with respect to its value at the step increase of temperature ( $t = 12 \text{ h}$ ). As a result, when drug release is switched on again ( $t = 24 \text{ h}$ ), the drug flux  $h_{dr}$  given by eq. (64) increases with respect to the value at drug release switch-off, as indicated by the slopes of the drug release percent profile in Figure 2.

### 6.2. Temperature-activated crawler

As a prototype of a temperature-activated crawler, we consider a hydrogel beam whose bottom surface is coated with a thin layer consisting of a thermo-responsive gel. The beam is  $L = 20$  mm long,  $b = 1$  mm wide and  $h_o = 2$  mm thick, including the thickness of the coating layer, which is  $\beta = 1/10$  of the total thickness. The material parameters are taken as in Table 1. The crawler interacts with a directional substrate (Hancock et al., 2012) that exerts a friction force sensitive only to the sign of the sliding velocity, that is, a directional dry-friction interaction (Gidoni et al., 2014; Noselli and DeSimone, 2014). In particular, the friction force for positive velocity is less than for negative velocity. The crawler is initially in free-swelling equilibrium with a pure liquid solvent ( $\mu_e = 0$  J/mol); the free-swelling stretches of the beam and the coating layer with respect to the dry configuration are  $\lambda_o$  and  $\lambda_{so}$ , respectively. For a time interval  $\tau$ , we prescribe a temperature profile that linearly increases from  $T_o = 298$  K to  $T_m = 300$  K, which corresponds to an increase in  $\chi_s$  from 0.2 to 0.4, in half cycle  $\tau/2$  and then linearly decreases to  $T_o$  in the remaining half cycle. As for the previous application, we assume that thermal equilibrium is instantaneous, thus neglecting transient heat transfer.

When temperature is increased from  $T_o$  to  $T_m$ , the coating layer shrinks, as solvent is expelled due to the reduction in the solvent-polymer chemical affinity, and the crawler bends. Because of the directional interaction with the substrate, the posterior edge of the beam that is in contact with the surface slides over it, while the anterior edge sticks to the substrate (Figure 3). As temperature is decreased to  $T_o$ , the crawler returns to its straight configuration as the coating layer swells, with the anterior edge sliding on the substrate and the posterior edge staying fixed. The sliding  $\Delta$  of the posterior edge in the first half of the cycle equals the advancement of the crawler in one temperature cycle, which is about  $L/10$ , for the crawler we are considering here.

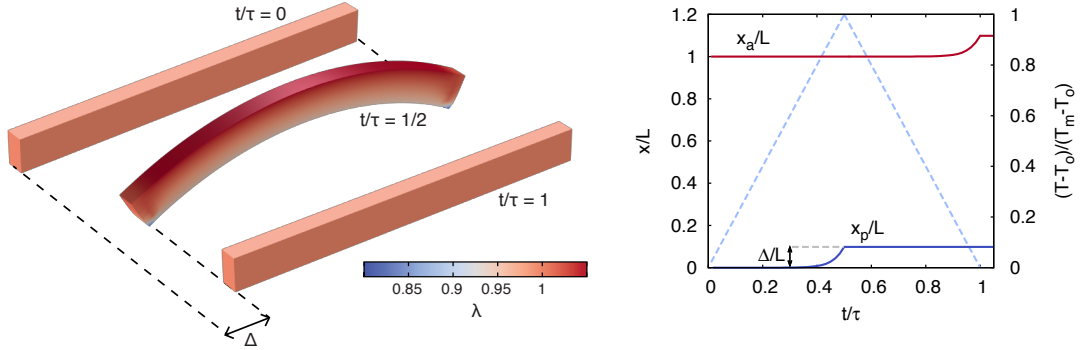


Figure 3: Motion of the temperature-activated crawler. (Left) Snapshots of the crawler advancing on a directional substrate by exploiting the dry friction. When temperature is increased from  $T_o$  to  $T_m$ , the crawler bends and the posterior edge in contact with the surface moves over it, while the anterior edge stays fixed. Color code represents the longitudinal stretch  $\lambda$  of the crawler. (Right) Dimensionless positions  $x_p/L$  and  $x_a/L$  of the posterior edge and of the anterior edge, respectively, as a function of the scaled time  $t/\tau$  during a period  $\tau$  corresponding to one temperature cycle. The dashed line is the temperature profile.

The longitudinal stretch and curvature of the longitudinal axis of the crawler can be estimated using a plane-bending model of a bilayer beam, as in (Lucantonio et al., 2014a). Under the assumption of plane cross-sections, we represent the longitudinal stretch of the beam as:

$$\lambda(z) = \Lambda_o(1 + z\Lambda_o\kappa), \quad (65)$$



where  $z \in [-h_o/2, h_o/2]$  is the thickness coordinate,  $\Lambda_o$  and  $\kappa$  are the (uniform) stretch and curvature of the longitudinal axis  $z = 0$ , respectively. We assume that the longitudinal stress in the beam is related to the difference between the actual stretch  $\lambda$  and the stretches  $\lambda^f$  and  $\lambda_s^f$  that each layer would attain if it was free to swell separately from the other layer. Hence, we employ the following simplified constitutive equations for the longitudinal stresses within the layers:

$$\sigma(z) = 3G \left( \frac{\lambda(z)}{\lambda^f} - 1 \right), \quad \left( -\frac{h_o}{2} + \beta h_o \right) < z < \frac{h_o}{2}, \quad (66)$$

$$\sigma_s(z) = 3G_s \left( \frac{\lambda(z)}{\lambda_s^f} - 1 \right), \quad -\frac{h_o}{2} < z < \left( -\frac{h_o}{2} + \beta h_o \right), \quad (67)$$

where  $\lambda^f$  and  $\lambda_s^f$  are determined by the free-swelling equilibrium equation (51):

$$\log \frac{(\lambda^f \lambda_o)^3 - 1}{(\lambda^f \lambda_o)^3} + \frac{1}{(\lambda^f \lambda_o)^3} + \frac{\chi}{(\lambda^f \lambda_o)^6} + \frac{G\Omega}{\mathcal{R}T} \frac{1}{\lambda^f \lambda_o} = \frac{\mu_e}{\mathcal{R}T}, \quad (68)$$

$$\log \frac{(\lambda_s^f \lambda_{so})^3 - 1}{(\lambda_s^f \lambda_{so})^3} + \frac{1}{(\lambda_s^f \lambda_{so})^3} + \frac{\chi_s}{(\lambda_s^f \lambda_{so})^6} + \frac{G_s\Omega}{\mathcal{R}T} \frac{1}{\lambda_s^f \lambda_{so}} = \frac{\mu_e}{\mathcal{R}T}, \quad (69)$$

By imposing that the force and moment resultants over the cross-section of the crawler vanish,

$$b \int_{-h_o/2}^{-h_o/2+\beta h_o} \sigma_s(z) dz + b \int_{-h_o/2+\beta h_o}^{h_o/2} \sigma(z) dz = 0, \quad (70)$$

$$b \int_{-h_o/2}^{-h_o/2+\beta h_o} z \sigma_s(z) dz + b \int_{-h_o/2+\beta h_o}^{h_o/2} z \sigma(z) dz = 0, \quad (71)$$

we obtain the following system of equations, with  $\Lambda_1 = \kappa \Lambda_o^2$ ,

$$\left( A \frac{G}{\lambda^f} + A_s \frac{G_s}{\lambda_s^f} \right) \Lambda_o + \left( S \frac{G}{\lambda^f} + S_s \frac{G_s}{\lambda_s^f} \right) \Lambda_1 = AG + A_s G_s, \quad (72)$$

$$\left( S \frac{G}{\lambda^f} + S_s \frac{G_s}{\lambda_s^f} \right) \Lambda_o + \left( I \frac{G}{\lambda^f} + I_s \frac{G_s}{\lambda_s^f} \right) \Lambda_1 = SG + S_s G_s, \quad (73)$$

where  $A, A_s$  are the areas of the cross-sections of the layers,  $S, S_s$  are the static moments of such cross-sections, and  $I, I_s$  are the moments of inertia. These equations, together with the free-swelling equations, provide the longitudinal stretch  $\Lambda_o$  and the curvature  $\kappa$  of the axis of the crawler. In Figure 4 we report the comparison among the solution of this system for different values of  $\chi_s$ , the numerical solution of the model where both the layers are treated as three-dimensional gels, and the numerical solution of the crawler model where the coating layer is modeled as a swelling material surface. We notice that for moderate curvatures, corresponding to values of  $\chi_s \leq 0.4$ , the agreement among the models is good, especially for the values of  $\Lambda_o$ , which stay within a 1% variation.

### 6.3. Spreading and absorption of a liquid on the surface of a gel layer

Surfaces of bodies usually display mechanical and diffusion properties that are different from those of bulk materials and affect surface transport processes. In particular, spreading and absorption phenomena over porous surfaces are important for many technological applications, such as high speed inkjet printing on coated papers (Kettle et al., 2010). Here we study an example problem where the surface of a gel layer (edge length  $L = 100 \mu\text{m}$ , thickness  $L/8$ ) has

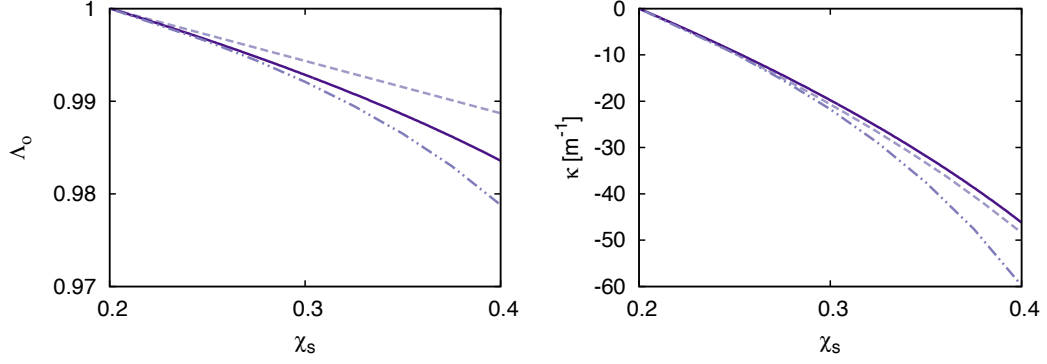


Figure 4: Comparison among the results obtained with several models of the crawler. Longitudinal stretch (left) and curvature (right) of the longitudinal axis of the crawler as a function of the dimensionless mixing parameter  $\chi_s$ . The dashed-dotted line is the result obtained with the analytical bilayer beam model, the solid line is the result obtained with the fully three-dimensional model, while the dashed line is the result obtained with the swelling material surface model introduced in this paper.

a different permeability to the solvent with respect to the bulk permeability. The surface is modeled as a swelling material surface, with a thickness  $h = 1 \mu\text{m}$ . A solvent flux is prescribed for  $\tau = 1 \text{ s}$  on a circular region with radius  $10 \mu\text{m}$  at the center of the surface. Over the period  $\tau$ , the flux is constant in time and the total amount of solvent absorbed by the layer equals  $V/8$ , where  $V$  is the volume of the gel layer. For the material parameters, we take  $G = G_s = 40 \text{ kPa}$ ,  $\Omega = 6 \times 10^{-5} \text{ m}^3/\text{mol}$ ,  $\chi = \chi_s = 0.2$ ,  $T = 298 \text{ K}$ ,  $D = 10^{-10} \text{ m}^2/\text{s}$ . The boundary diffusivity  $D_s$  varies between  $D$  and  $10^3 D$ .

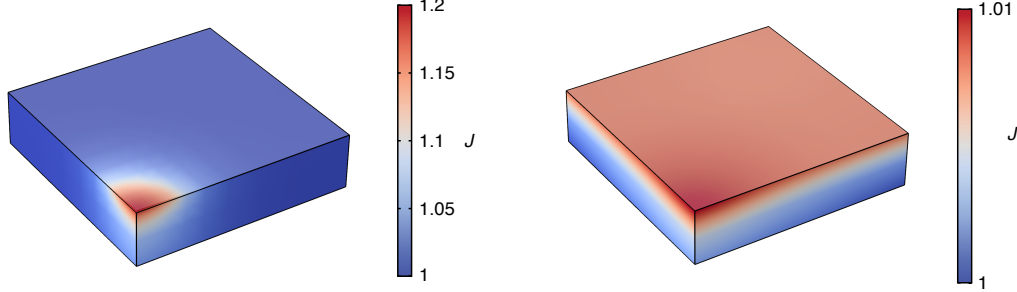


Figure 5: A gel layer coated with a surface having a different solvent permeability. A solvent flux is prescribed for  $1 \text{ s}$  in a circular region at the center of the layer. The solvent partially spreads over the surface and is also absorbed by the layer. Plot of the swelling ratio  $J$  at time  $t = 1 \text{ s}$  over  $1/4$  of the gel layer for (left)  $D_s = 1 \times 10^{-10} \text{ m}^2/\text{s} = D$  and for (right)  $D_s = 1 \times 10^{-7} \text{ m}^2/\text{s}$ .

The results of the numerical simulations corresponding to different values of  $D_s$  are reported in Figure 5. When  $D = D_s$ , solvent migration along the thickness, *i.e.* solvent absorption, is faster than in the in-plane directions, because the diffusion time scale, which is proportional to the square of a characteristic length, is smaller along the thickness. As  $D_s$  increases, surface spreading, *i.e.* in-plane solvent transport, prevails on transport along the thickness, so that the solvent profile tends to homogenize in the plane faster than the transport along the thickness.

## 7. Conclusions

In this paper, we have established a thermodynamically consistent theory for swelling material surfaces that allows to describe the coupled elasticity and solvent transport in polymer gel membranes. The balance equations for the swelling material surface have been obtained from a virtual work functional, following a direct approach, instead of performing a dimensional reduction from a three-dimensional parent theory. A kinematical constraint relating the change in solvent content of the swelling membrane to its volume change and a surface energy for the swelling material surface consistent with the Flory-Rehner theory have been derived.

We have applied the theory to the study of several model problems motivated by technological applications in the fields of biomedicine, micro-motility and coating technology. Specifically, we have studied a smart drug delivery system, a temperature-activated micro-crawler and a coated gel layer subject to surface spreading and absorption. We believe that the theory we have presented may be employed as an effective tool in the design of such systems.

## Acknowledgments

AL acknowledges support of Regione Friuli Venezia Giulia through Fondo Sociale Europeo – S.H.A.R.M. project and thanks Giovanni Noselli for useful discussions. ADS acknowledges support of European Research Council through the ERC Advanced Grant 340685 – MicroMotility.

## References

- Antman, S.S., 2005. *Nonlinear Problems of Elasticity*. Springer.
- Bae, Y.H., Okano, T., Kim, S.W., 1991. “on-off” thermocontrol of solute transport. ii. solute release from thermosensitive hydrogels. *Pharmaceutical Research* 8, 624–628. URL: <http://dx.doi.org/10.1023/A%3A1015860824953>, doi:10.1023/A:1015860824953.
- Capriz, G., 1989. *Continua with Microstructure*. Springer-Verlag.
- Chester, S.A., Anand, L., 2011. A thermo-mechanically coupled theory for fluid permeation in elastomeric materials: Application to thermally responsive gels. *Journal of the Mechanics and Physics of Solids* 59, 1978 – 2006. URL: <http://www.sciencedirect.com/science/article/pii/S0022509611001426>, doi:<http://dx.doi.org/10.1016/j.jmps.2011.07.005>.
- DiCarlo, A., Podio-Guidugli, P., Williams, W., 2001. Shells with thickness distension. *International Journal of Solids and Structures* 38, 1201–1225. URL: <http://www.sciencedirect.com/science/article/pii/S0020768300000822>, doi:[http://dx.doi.org/10.1016/S0020-7683\(00\)00082-2](http://dx.doi.org/10.1016/S0020-7683(00)00082-2).
- Ganghoffer, J.F., Haussy, B., 2005. Mechanical modeling of growth considering domain variation. part i: constitutive framework. *International Journal of Solids and Structures* 42, 4311–4337. URL: <http://www.sciencedirect.com/science/article/pii/S0020768305000235>, doi:10.1016/j.ijsolstr.2005.01.011.
- Germain, P., 1973. The method of virtual power in continuum mechanics. part 2: Microstructure. *SIAM Journal on Applied Mathematics* 25, 556–575. URL: <http://epubs.siam.org/doi/abs/10.1137/0125053>, doi:10.1137/0125053.

- Gidoni, P., Noselli, G., DeSimone, A., 2014. Crawling on directional surfaces. *International Journal of Non-Linear Mechanics* 61, 65–73. URL: <http://www.sciencedirect.com/science/article/pii/S0020746214000213>, doi:10.1016/j.ijnonlinmec.2014.01.012.
- Gurtin, M.E., Murdoch, I.A., 1975. A continuum theory of elastic material surfaces. *Archive for Rational Mechanics and Analysis* 57, 291–323. doi:10.1007/BF00261375.
- Hancock, M.J., Sekeroglu, K., Demirel, M.C., 2012. Bioinspired directional surfaces for adhesion, wetting, and transport. *Advanced Functional Materials* 22, 2223–2234. URL: <http://dx.doi.org/10.1002/adfm.201103017>, doi:10.1002/adfm.201103017.
- Hoare, T.R., Kohane, D.S., 2008. Hydrogels in drug delivery: Progress and challenges. *Polymer* 49, 1993–2007. URL: <http://linkinghub.elsevier.com/retrieve/pii/S0032386108000487>, doi:10.1016/j.polymer.2008.01.027.
- Holmes, D.P., Roché, M., Sinha, T., Stone, H.A., 2011. Bending and twisting of soft materials by non-homogenous swelling. *Soft Matter* 7, 5188–5193. doi:10.1039/C0SM01492C.
- Hu, Z., Chen, Y., Wang, C., Zheng, Y., Li, Y., 1998. Polymer gels with engineered environmentally responsive surface patterns. *Nature* 393, 149–152. URL: <http://www.nature.com/nature/journal/v393/n6681/full/393149a0.html>, doi:10.1038/30205.
- Ionov, L., 2011. Soft microorigami: self-folding polymer films. *Soft Matter* 7, 6786. URL: <http://xlink.rsc.org/?DOI=c1sm05476g>, doi:10.1039/c1sm05476g.
- Javili, A., McBride, A., Steinmann, P., Reddy, B., 2014. A unified computational framework for bulk and surface elasticity theory: a curvilinear-coordinate-based finite element methodology. *Computational Mechanics* 54, 745–762. URL: <http://dx.doi.org/10.1007/s00466-014-1030-4>, doi:10.1007/s00466-014-1030-4.
- Kettle, J., Lamminmäki, T., Gane, P., 2010. A review of modified surfaces for high speed inkjet coating. *Surface and Coatings Technology* 204, 2103–2109. URL: <http://linkinghub.elsevier.com/retrieve/pii/S0257897209008433>, doi:10.1016/j.surfcoat.2009.10.035.
- Kikuchi, A., Okano, T., 2002. Pulsatile drug release control using hydrogels. *Advanced drug delivery reviews* 54, 53–77. URL: <http://www.sciencedirect.com/science/article/pii/S0169409X01002435>.
- Kim, J., Hanna, J.a., Byun, M., Santangelo, C.D., Hayward, R.C., 2012. Designing responsive buckled surfaces by halftone gel lithography. *Science* 335, 1201–1205. URL: <http://www.ncbi.nlm.nih.gov/pubmed/22403385>, doi:10.1126/science.1215309.
- Klein, Y., Efrati, E., Sharon, E., 2007. Shaping of elastic sheets by prescription of non-euclidean metrics. *Science* 315, 1116–1120. URL: <http://www.sciencemag.org/cgi/doi/10.1126/science.1135994>, doi:10.1126/science.1135994.
- Libai, A., Simmonds, J.G., 1998. *Nonlinear theory of elastic shells*. Cambridge University Press.
- Lucantonio, A., Nardinocchi, P., 2012. Reduced models of swelling-induced bending of gel bars. *International Journal of Solids and Structures* 49, 1399–1405. doi:10.1016/j.ijsolstr.2012.02.025.

- Lucantonio, A., Nardinocchi, P., Pezzulla, M., 2014a. Swelling-induced and controlled curving in layered gel beams. *Proceedings of the Royal Society A: Mathematical, Physical and Engineering Science* 470. URL: <http://rspa.royalsocietypublishing.org/content/470/2171/20140467.abstract>, doi:10.1098/rspa.2014.0467.
- Lucantonio, A., Nardinocchi, P., Stone, H.A., 2014b. Swelling dynamics of a thin elastomeric sheet under uniaxial pre-stretch. *Journal of Applied Physics* 115, 083505. URL: <http://scitation.aip.org/content/aip/journal/jap/115/8/10.1063/1.4866576>.
- Lucantonio, A., Nardinocchi, P., Teresi, L., 2013. Transient analysis of swelling-induced large deformations in polymer gels. *Journal of the Mechanics and Physics of Solids* 61, 205–218. doi:10.1016/j.jmps.2012.07.010.
- Lucantonio, A., Roché, M., Nardinocchi, P., Stone, H.A., 2014c. Buckling dynamics of a solvent-stimulated stretched elastomeric sheet. *Soft Matter* 10, 2800. URL: <http://xlink.rsc.org/?DOI=c3sm52941j>, doi:10.1039/c3sm52941j.
- McBride, A., Javili, A., Steinmann, P., Bargmann, S., 2011. Geometrically nonlinear continuum thermomechanics with surface energies coupled to diffusion. *Journal of the Mechanics and Physics of Solids* 59, 2116 – 2133. URL: <http://www.sciencedirect.com/science/article/pii/S002250961100127X>, doi:http://dx.doi.org/10.1016/j.jmps.2011.06.002.
- Murdoch, A.I., 1990. A coordinate-free approach to surface kinematics. *Glasgow Mathematical Journal* 32, 299–307. URL: [http://journals.cambridge.org/abstract\\_S0017089500009381](http://journals.cambridge.org/abstract_S0017089500009381).
- Noselli, G., DeSimone, A., 2014. A robotic crawler exploiting directional frictional interactions: experiments, numerics and derivation of a reduced model. *Proceedings of the Royal Society of London A: Mathematical, Physical and Engineering Sciences* 470. doi:10.1098/rspa.2014.0333.
- Ottenbrite, R.M., Park, K., Okano, T. (Eds.), 2010. *Biomedical Applications of Hydrogels Handbook*. Springer.
- Pandey, A., Holmes, D.P., 2013. Swelling-induced deformations: a materials-defined transition from macroscale to microscale deformations. *Soft Matter* 9, 5524. URL: <http://xlink.rsc.org/?DOI=c3sm00135k>, doi:10.1039/c3sm00135k.
- Peppas, N.A., Bures, P., Leobandung, W., Ichikawa, H., 2000. Hydrogels in pharmaceutical formulations. *European journal of pharmaceuticals and biopharmaceutics* 50, 27–46. URL: <http://www.sciencedirect.com/science/article/pii/S0939641100000904>.
- Sawa, Y., Urayama, K., Takigawa, T., DeSimone, A., Teresi, L., 2010. Thermally driven giant bending of liquid crystal elastomer films with hybrid alignment. *Macromolecules* 43, 4362–4369. URL: <http://dx.doi.org/10.1021/ma1003979>, doi:10.1021/ma1003979.
- Siepmann, J., Siepmann, F., 2012. Modeling of diffusion controlled drug delivery. *Journal of Controlled Release* 161, 351 – 362. URL: <http://www.sciencedirect.com/science/article/pii/S0168365911009588>, doi:http://dx.doi.org/10.1016/j.jconrel.2011.10.006. drug Delivery Research in Europe.
- Starov, V.M., Zhdanov, S.A., Velarde, M.G., 2002. Spreading of liquid drops over thick porous layers: Complete wetting case. *Langmuir* 18, 9744–9750. URL: <http://dx.doi.org/10.1021/la025759y>, doi:10.1021/la025759y.

- Steinmann, P., McBride, A., Bargmann, S., Javili, A., 2012. A deformational and configurational framework for geometrically non-linear continuum thermomechanics coupled to diffusion. *International Journal of Non-Linear Mechanics* 47, 215–227. URL: <http://linkinghub.elsevier.com/retrieve/pii/S0020746211001077>, doi:10.1016/j.ijnonlinmec.2011.05.009.
- Stuart, M.A.C., Huck, W.T.S., Genzer, J., Müller, M., Ober, C., Stamm, M., Sukhorukov, G.B., Szleifer, I., Tsukruk, V.V., Urban, M., Winnik, F., Zauscher, S., Luzinov, I., Minko, S., 2010. Emerging applications of stimuli-responsive polymer materials. *Nature Materials* 9, 101–113. URL: <http://www.nature.com/nmat/journal/v9/n2/full/nmat2614.html>, doi:10.1038/nmat2614.
- Wu, Z.L., Moshe, M., Greener, J., Therien-Aubin, H., Nie, Z., Sharon, E., Kumacheva, E., 2013. Three-dimensional shape transformations of hydrogel sheets induced by small-scale modulation of internal stresses. *Nature Communications* 4, 1586. URL: <http://www.nature.com/doi/10.1038/ncomms2549>, doi:10.1038/ncomms2549.